THE OPTIC INTERFERENCE FIGURES OF AMETHYSTINE QUARTZ—PART II

BY S. PANCHARATNAM

(*Memoir No.* 107 *of the Raman Research Institute, Bangalore-6*)

Received on April 9, 1958

(Communicated by Sir C. V. Raman)

§1. INTRODUCTION

IN the remaining part of the paper, observations on the interference figures of the amethystine sector are continued, using a wavelength lying in the heart of the absorption band (λ 5890). Here the effects of dichroism gain such ascendancy ($k > 2 \mid \rho \mid$) that the existence of optical rotatory power is itself only indirectly manifested—through the exceptional nature of the observed phenomena.

§2. OBSERVATIONS BETWEEN CROSSED POLAROIDS

Figures 1–6 (Plate XI) demonstrate the singular behaviour of the isogyres observed between *crossed* polaroids as the latter are turned around *together* in a clockwise sense—starting with the setting in which the vibration-direction of the polariser is parallel to the axial plane. (The settings of polariser and analyser have been respectively marked in the upper and lower circles drawn by the side of each figure, the axial directions themselves being marked by white dots in some of the photographs.) *There are only two settings of the incident vibration, viz.*, when it is parallel to either $O'A_1$ or $O'A_2$ in Fig. 1, text, *for which genuine isogyres are observed* passing unmodified through the two optic axes, as seen in Figs. 2 and 3 (Plate XI). For all other settings of the crossed polaroids it was observed that the 'isogyres' appeared really dark only towards the border of the figure. This is true even in Figs. 5 and 6 though the crossed polaroids are in orientations obtained merely by interchanging the polariser and analyser in the settings of Figs. 2 and 3 respectively.

§ 3. PROPERTIES OF THE OPTIC AXES

The observations of the previous paragraph clearly mean that when the incident vibration is parallel to either $O'A_1$ or $O'A_2$ (Fig. 1, text) it is propagated without resolution along each axial direction. We thus arrive experimentally at the conclusion that *the waves propagated along an optic axis, e.g.*, along O_1, *are linearly polarised along two non-orthogonal directions*

parallel to $O'A_1$ and $O'A_2$, as marked at O_1 in Fig. 1, text. These directions are found to be equally inclined to the lines bisecting the angle between $O'X_k$ and $O'Y_k$, and lie in the negative quadrant. These results are exactly what have been already derived* theoretically in P–a^1, §8 *b*, for the propagation along an axial direction when the dichroism is sufficiently large ($k > |2\rho|$). For the purpose of discussion it is convenient to refer to Fig. 2 *a* text, which represents a plate cut exactly normal to an optic axis on which have been marked the principal planes of linear dichroism OX_k and OY_k. The linearly polarised states P_a and P_b of the waves that can be propagated normal to the plate should both lie in the negative quadrant (since ρ is negative) at azimuths whose numerical values ψ_1 and $(\frac{1}{2}\pi - \psi_1)$ are the roots of

$$\tfrac{1}{2}k \sin 2\psi = |\rho| \qquad (1)$$

Furthermore, these waves should differ not in their velocities, but only in their coefficients of absorption k_a and k_b:

$$(k_b - k_a) = k \cos 2\psi_1 \qquad (2)$$

When the vibration incident along an axial direction is in a general setting (*i.e.*, other than $O'A_1$ or $O'A_2$), it will be decomposed into two non-orthogonal vibrations in states P_a and P_b according to the parallelogram law (*see e.g.*, reference 2, Fig. 3); while according to the same law the attenuated vibrations emerging from the plate should compound to yield a linear vibration whose azimuth would have turned towards the plane of the less attenuated state P_a. In accordance with this it was always found possible to extinguish the optic axial directions by turning the analyser away from the crossed position. This is illustrated in Figs. 7 and 8 (Plate XII); in Fig. 7 the angles that the vibration-directions of the polariser and analyser made with respect to $O'X_k$ were $-59°$ and $+59°$ respectively; while for Fig. 8 the corresponding angles were $-84\frac{1}{2}°$ and $+84\frac{1}{2}°$. A straightforward calculation—based on the explanation given above of the extinction of the optic axes—enables the difference in the absorption coefficients of the waves propagated along an axial direction to be estimated. If d be the thickness of the plate, it is easily shown that for an axial direction $(k_b - k_a)\,d$ is equal to 2·5, this being the mean of the two values calculated from the settings of Figs. 7 and 8 respectively. The angle between $O'A_1$

* These results may also be derived analytically by directly applying the principle of superposition. Thus, if both sides of (1) be multiplied by dz, the left-hand side and right-hand side denote respectively the angles through which a plane vibration at azimuth ψ turns during the infinitesimal operations of dichroism and rotation respectively; for these to be equal and opposite, eq. (1) should be satisfied, and the plane of vibration should lie in the negative quadrant, if ρ is negative.

and $O'A_2$ (*i.e.*, between the settings of the polariser in Figs. 2 and 3) was required in the calculation; it was estimated to be 50°, this being done more accurately from observations using a polariser alone and an analyser alone (§8). (It may be noted that this angle may also be *calculated* by measuring the turning of the plane of polarisation along the axial directions for *two* azimuths of the incident vibration, as in Figs. 7 and 8.) We then obtain $kd = 3{\cdot}25$ from (2), giving an estimate of the 'pure' linear dichroism.

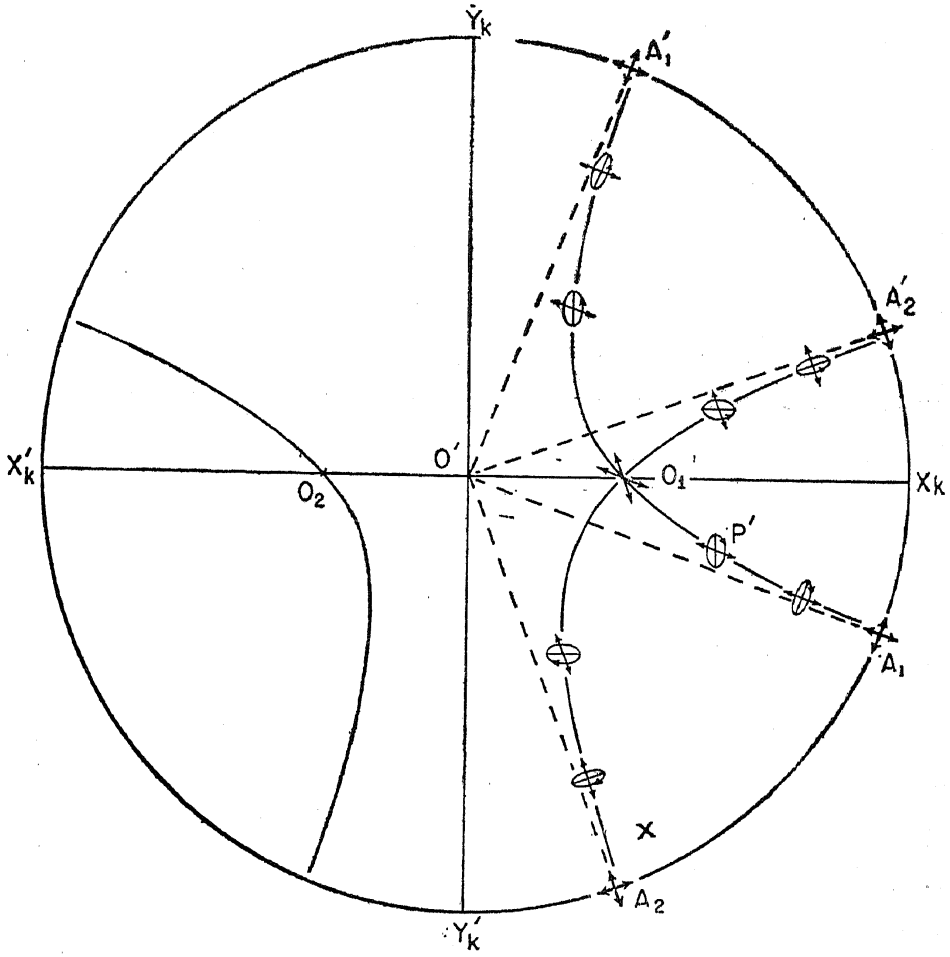

TEXT-FIG. 1. Convergent light figure depicting the variation of the states of polarisation of the waves with the direction of propagation for particular zones in the field of view. O_1 and O_2 are the optic axes.

The optical rotatory power along the axial directions—though masked by the effects of dichroism—may now be indirectly estimated by substituting the values $\psi_1 = 20°$, and $kd = 3{\cdot}25$ in (1). The total optical rotation $|\rho|\,d$ (which would be exhibited along the axial directions in the absence of dichroism) turns out to be about 59·5°—after conversion from radians to degrees. Since this is practically the same as the rotation for a plate of transparent

quartz of the same thickness (*viz.*, 2·8 mm.), we have here a semi-quantitative check on the results of our theory.

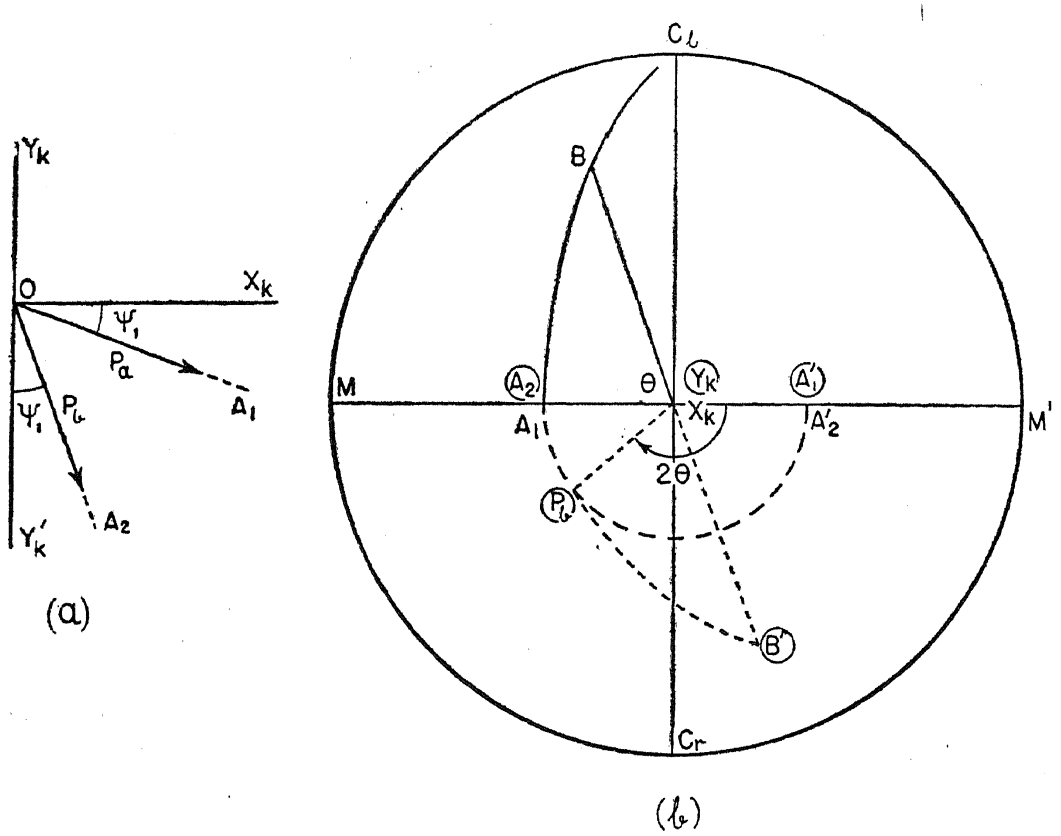

TEXT-FIG. 2. (*a*) Plate cut normal to an optic axis along which the waves propagated are linearly polarised in non-orthogonal states P_a and P_b.

(*b*) Construction on the Poincaré sphere determining the points A_1 and P_b which represent the states propagated unchanged along the direction P′ of Fig. 1, Text.

§4. EXPLANATION OF THE FORMATION OF ISOGYRES

We now turn to the fact that in Fig. 2 for example—where the vibration-direction of the polariser is parallel to $O'A_1$ (Fig. 1, text)—it is not the two optic axial directions *alone* that are extinguished; all the directions represented by points on the dark isogyres are extinguished (in sharp contrast to the behaviour of transparent active crystals). These isogyres form a rectangular hyperbola (with $O'A_1$ and $O'A_1'$ as asymptotes) one branch of which has been marked $A_1O_1A'_1$ in Fig. 1, text. We may conclude from our observation that along any direction represented by a point on this hyperbola (*e.g.*, the point P′), a vibration parallel to $O'A_1$ can be propagated unchanged—so as to be completely extinguished by the crossed analyser; while for the same direction P′ a vibration parallel to $O'A_1'$ is *not* propagated

unchanged—as is shown by the absence of isogyres in Fig. 5, obtained by interchanging the polariser and analyser settings of Fig. 2.

This conclusion may be theoretically explained by the method of superposition presented in P–*a*: for a general direction of propagation we will observe the superposed effects not only of linear dichroism and optical rotation (as along the axial directions) but also of the linear birefringence which would be present even in a transparent inactive crystal. The clue to the explanation of the isogyres which form when the vibration-direction of the polariser is parallel to $O'A_1$ (Fig. 1, text) is given by the fact that the isogyres (one branch of which is marked $A_1O_1A_1'$) would have occurred in the same position even in the absence of optical activity and linear dichroism (*see e.g.*, Johannsen[3]). That is to say, any point such as P′ lying on these isogyres represents a direction for which one of the principal planes of linear birefringence lies parallel to $O'A_1$. Hence, for such a direction a vibration parallel to $O'A_1$ will remain unchanged under the effect of the infinitesimal operation of linear birefringence. The same vibration will also remain unaltered under the *combined* effects of the two succeeding infinitesimal operations of linear dichroism and optical rotation—as is evidenced by the fact that it is propagated unchanged along the axial directions where these two factors alone subsist (§3). It follows that a vibration parallel to $O'A_1$ can be propagated unaltered (along the zone of directions represented by the isogyres) under the combined effect of all three factors, *viz.*, linear birefringence, linear dichroism and optical rotation. It may be similarly proved that a vibration parallel to $O'A_1'$ cannot be propagated unchanged along these directions; for it is *not* propagated unchanged under the combined effects of the second two factors alone—as is evidenced by the fact that it is not propagated unchanged along an axial direction. This explains the presence of genuine isogyres in Fig. 2 and their absence in Fig. 5.

The isogyres in Fig. 3 form a rectangular hyperbola—with asymptotes $O'A_2$ and $O'A_2'$—one branch of which has been marked $A_2O_1A_2'$. It may be shown by an exactly similar argument that along the zone of directions represented by this hyperbola a vibration parallel to $O'A_2$ can be propagated unchanged, but not a vibration parallel to $O'A_2'$; this explains the presence of genuine isogyres in Fig. 3 and their absence in Fig. 6.

The main result of this section may be summarised in a form applicable to crystals of arbitrary axial angle and of any symmetry (in a region where $k > |2\rho|$). *Isogyres are formed between crossed polaroids only when the polariser setting is parallel to one of the vibration-directions of the waves propagated along an optic axis*; the isogyres then occupy the same position

as they would in a transparent inactive crystal with the same axial directions. It is, of course, assumed that the optical rotatory power and linear dichroism do not vary rapidly in the neighbourhood of the optic axis considered.

§5. States of Polarisation of the Waves

(*a*) *Co-ordinates for points in convergent light figure.*—We shall now see what will be the states of polarisation of the waves propagated along the direction represented by the arbitrary point P in the convergent light figure (Fig. 3 *a*, text). In the present case, it is best to specify the point P in curvilinear co-ordinates δ, χ. In the region of view in Fig. 3 *a*, text, we can draw two families of intersecting curves. The point P has been depicted as the point of intersection of two of these curves. The first is a curve of constant linear birefringence characterised by the parameter δ which is equal to the linear birefringence, *i.e.*, the birefringence in the absence of optical activity and linear dichroism; this curve takes the form of an 'oval of Cassini' (*see e.g.*, Wooster[4]). The second curve is a branch of a rectangular hyperbola which is drawn passing through the two optic axes, having as its asymptotes two perpendicular lines O'L and O'L' drawn through the centre of the figure. This hyperbola really represents a curve of like polarisation in the absence of optical activity and linear dichroism, since it would then represent the position of the isogyres formed when the crossed polaroids are set parallel to O'L and O'L' (*see* Johannsen[3]). The hyperbolic segment O_1PL may be characterised by the parameter χ, where $(-\chi)$ is the angle that its asymptote O'L makes with respect to $O'X_k$. For any point on this hyperbolic segment χ the principal plane of linear birefringence OX_r (corresponding to the slower wave in the absence of optical activity and dichroism) makes an angle $-\chi$ with $O'X_k$.

For a point in the convergent light figure which is related to P by inversion about the central point O', the orientation of the principal planes of linear birefringence, as well as the magnitude of the linear birefringence will be the same as for the point P itself. All other factors being taken to be constant over the field of view, *the interference figures in convergent light must always be centrosymmetric about O'*. That this is not strictly what is observed (*see e.g.*, Brewster's brushes, Part I, Fig. 5, Plate IX) is mainly because the coefficients of linear dichroism exhibit some variation over the field of view. For the sake of our qualitative discussion we may neglect this variation. Accordingly *it is sufficient to consider only the field of view on the right of the vertical line* Y_kY_k'.

(*b*) *Approximate discussion.—For directions of propagation lying towards the border of the figure*, the variation of the states of polarisation of the two

waves as we proceed round a curve of constant linear birefringence δ may be easily studied in a fairly comprehensive manner. The two waves propagated along the direction P will be elliptically polarised; and according to the approximate results of P–*a*[1], §7 *b*, we may take the major axes of the

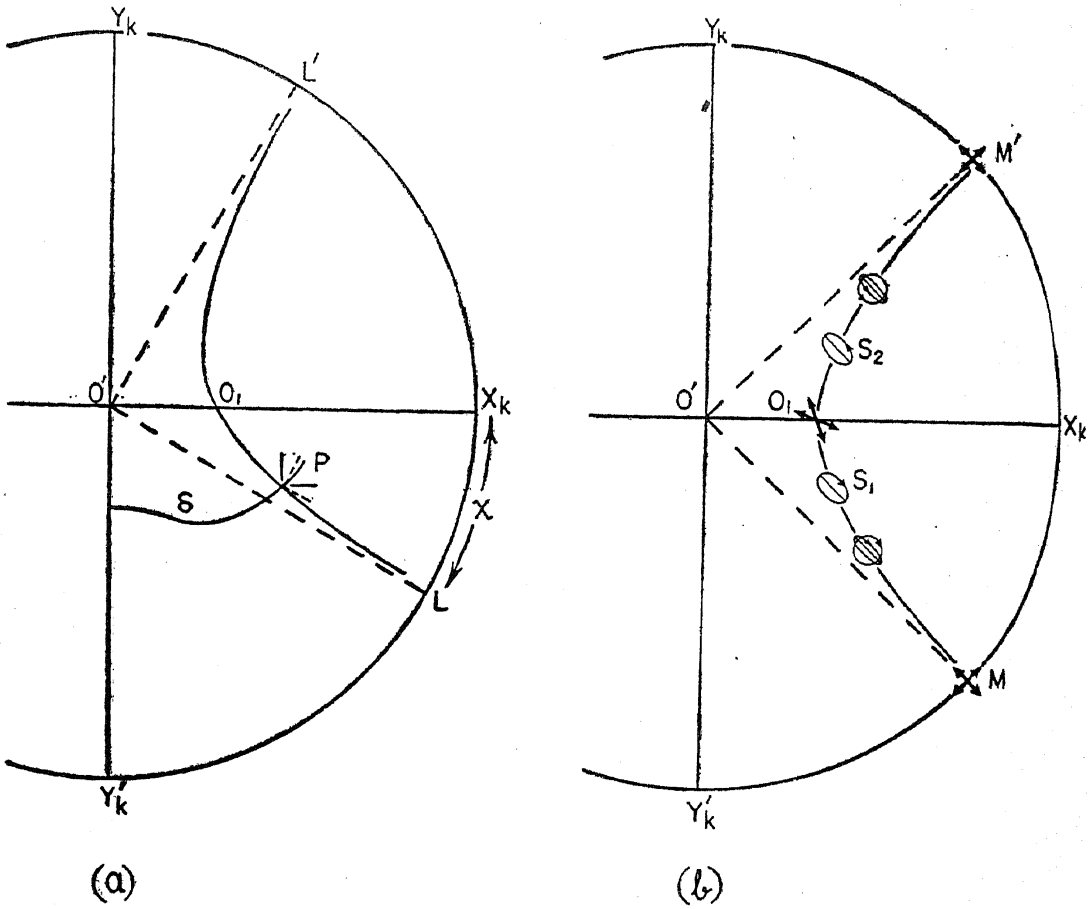

TEXT–FIG. 3. (*a*) Curvilinear co-ordinates (δ, χ) for the point P in the convergent light figure. (*b*) States of polarisation of the waves propagated along directions represented by points on MO_1M'; S_1 and S_2 are the singular axes.

slower and faster ellipses to lie along the corresponding principal planes of linear birefringence (OX_τ and OY_τ); and if ω represent the ellipticity of one of these elliptically polarised waves propagated along P (δ, χ), then since ρ is negative in the present case,

$$\omega = \pm \mid \rho \mid /\delta - \tfrac{1}{2}k \sin 2\chi/\delta \qquad (3)\dagger$$

the first term being taken with a positive or negative sign according as the ellipticity of the slower or faster wave is required.

† We had inadvertantly omitted, in P–*a*, eq. 15, to include a negative sign before the expression for ϵ, the common ellipticity of the waves in the absence of optical activity.

The variation of the ellipticity of the waves with direction (for points near the border of the figure) may be obtained from (3). We shall not proceed to describe this variation, since for such directions, the ellipticity is so small, that any experimental test using elliptically polarised light becomes difficult. It is to be noted that (3) may also be used for discussing the propagation for wavelengths in the red (where $k < |2\rho|$). But a characteristic difference which arises only in the present case (where yellow light is used) may be mentioned: there exists a zone of directions, *viz.*, those included between the segments O_1A_2 and O_1A_1 as also those between O_1A_2' and O_1A_1', for which both ellipses have the same sense of description—this common sense of description being the same as that in an inactive absorbing crystal.

(*c*) *General direction of propagation.*—The principal planes of linear birefringence and linear dichroism corresponding to the direction P have been marked at P itself in Fig. 3 *a*, text, while they have also been marked in P–*a*, Fig. 1 *a*, for a plate cut normal to the direction represented by P. The states of elliptic polarisation of the waves propagated along the general direction P (δ, χ) may now be accurately determined using the results proved in P–*a* which we may briefly recapitulate.

The horizontal and vertical directions will be represented on the Poincaré sphere by two opposite points X_k and Y_k on the equator—the diameter $X_k Y_k$ being kept perpendicular to the paper in our diagrams. From the theory for transparent active crystals we may regard as given (*a*) the elliptic birefringence Δ in the absence of dichroism, (*b*) the diametrically opposite points B and B′ which represent the states of elliptic polarisation of the slower and faster waves propagated along the direction P in the absence of dichroism (*vide* P–*a*, Fig. 2 and §3 *a*). The states of polarisation of the waves actually propagated in the direction P (*i.e.*, with linear dichroism present) will be represented on the Poincaré sphere by two points P_a and P_b which we wish to determine. Now the angular distances $2\psi_a$ and $2\phi_a$ of the slower state P_a from X_k and B are also the angular distances of P_b from the opposite points Y_k and B′; and further, P_a and P_b lie on the same side of the great circle passing through X_k and B—the hemisphere on which they lie being fixed by the fact that the vertices B, P_a and X_k describe the triangle BP_aX_k in a positive sense. Because of this relation it becomes sufficient to locate geometrically the position of P_a; this may be done from the following additional features regarding the triangle BP_aX_k; (*i*) the angle at P_a is a right angle; (*ii*) the ratio of the sines of the angular distances $2\phi_a$ and $2\psi_a$ of P_a from B and X_k is equal to k/Δ. The absorption

coefficients and refractive indices of the states P_a and P_b are given by P–*a*, Eqns. 9 and 12.

The region of the convergent light figure which need be theoretically studied is considerably reduced by the following relation which may be proved from the results of P–*a*. The points on the Poincaré sphere, representing the states of polarisation of the waves propagated along the direction $P(\delta, \chi - \frac{1}{2}\pi)$ are obtained from those representing the states propagated along $P(\delta, \chi)$, by reflection about the equatorial plane of the sphere: the refractive indices of the states are interchanged after reflection but not the absorption coefficients. So also the points on the Poincaré sphere representing the states propagated along $P(\delta, \frac{1}{2}\pi - \chi)$ may be obtained from those representing the states propagated along $P(\delta, \chi)$ by reflection about the plane C_lMC_r: the absorption coefficients of the states are interchanged after reflection but not the refractive indices. We shall proceed to apply the results quoted in this sub-section to discuss in detail the propagation along particular zones of directions.

§6. Observations with Elliptically Polarised Light

Let us now consider a direction of propagation such as P′ lying on the hyperbolic segment O_1A_1 (Fig. 1, text). For such a direction the principal plane of linear birefringence OX_r lies parallel to $O'A_1$ and is represented on the Poincaré sphere by the point A_1 on the equator (*see* Fig. 2 *b*, text). The point B representing the state of polarisation of the slower wave in the absence of absorption, will lie on the meridian A_1C_l—since this state will be left-elliptically polarised with its major axis parallel to $O'A_1$. In §4 we have seen that a vibration parallel to $O'A_1$ is propagated unchanged along the direction P′ in the convergent light figure. Hence the point P_a—representing the state of polarisation of one of the waves propagated in this direction—coincides with A_1. The state P_a being given, the state P_b may be immediately located as described in §5 *c*. Thus since the arc P_bY_k should be equal to arc A_1X_k *the state* P_b *must lie on the dotted small circle* of angular radius Y_kA_2 drawn about Y_k as centre. Further P_b and A_1 should lie on the same side of the great circle drawn through B, X_k and B′, and arc P_bB' should be equal to arc A_1B. From the symmetry of the figure, P_b is clearly determined by the point of intersection of the dotted small circle (mentioned above) with the arc Y_kP_b which is drawn at an angle 2θ to the equator as indicated, θ being the angle A_1X_kB. Turning to the convergent light figure (Fig. 1, text) suppose the point P′ on which we have fixed our attention moves outwards from the optic axis O_1 along the hyperbolic segment O_1A_1; the state of elliptic polarisation B (which would have been propagated along

the direction P′ as the slower wave *in the absence of absorption*) changes progressively from a left-circular vibration (for P′ coinciding with the optic axis O_1) towards the state of a linear vibration parallel to $O'A_1$: that is, on the Poincaré sphere (Fig. 2 *b*, text) the point B moves down from C_l towards A_1 along the arc C_lA_1, θ decreasing from $\frac{1}{2}\pi$ to zero. At the same time the state P_b of the faster wave being determined by the angle 2θ moves from A_2 towards A_1' along the dotted small circle whose diameter is A_2A_1' (the locus of P_b being in the lower hemisphere).

We shall now express the above results in physical terms. For all points on the hyperbolic segment O_1A_1 the state of polarisation P_a of the slower wave remains linearly polarised parallel to $O'A_1$ (§4). But as we proceed outwards from the optic axis O_1 along this hyperbolic segment, the state of polarisation P_b of the faster wave progressively alters in a manner which may be described thus: the state P_b—which is initially linearly polarised parallel to $O'A_2$—opens out into a right-elliptic vibration the ellipticity of which initially increases, the major axis at the same time turning rapidly towards the direction $O'A_1'$ orthogonal to $O'A_1$; further out the ellipticity again decreases though the turning of the major axis towards $O'A_1'$ continues, so that towards the border of the figure the states of the two waves approximate to those given in §5 *b*—and thence towards vibrations linearly polarised along the principal planes of linear birefringence (*see* Fig. 1, text).

As we proceed outwards from the optic axial direction O_1 along the hyperbolic segment O_1A_1', the state P_b of the faster vibration will, on the Poincaré sphere, remain fixed at A_1: but the state P_a of the slower vibration may be shown (by a similar analysis) to move from A_2 towards A_1' along the arc of a small circle which again has A_1A_2' as diameter, but which now lies in the *upper* hemisphere. So also, as we proceed along the hyperbolic branch $A_2O_1A_2'$ from A_2 to A_2', the state of polarisation of *one* of the waves will, according to §4, remain fixed at A_2 on the Poincaré sphere. (This state represents the slower state for points on the segment O_1A_2 but becomes the faster state for points on segment O_1A_2'). At the same time the state of the other wave moves on the Poincaré sphere from A_2' to A_1 and back to A_2' tracing (in a clockwise sense) the small circle of diameter $A_2'A_1$. (The results of this paragraph follow from those quoted at the end of §5*c*.) The variation of the states of polarisation of the waves for points on the hyperbolic branches $A_1O_1A_1'$ and $A_2O_1A_2'$ has been illustrated in Fig. 1, text.

According to a well-known property of the Poincaré sphere, the elliptic state P_b in Fig. 2 *b*, text, may be produced by passing a linear vibration in the state A_1' through a mica plate of retardation 2θ whose slow

vibration-direction is represented by X_k; *i.e.*, by passing light first through a polaroid whose vibration-direction is parallel to $O'A_1'$ and then through a retardation plate whose slow vibration is parallel to the axial plane. In Fig. 9 this arrangement was kept in front of the crystal plate, while behind the crystal plate was placed an 'elliptic analyser' which was kept automatically crossed with respect to the elliptic polariser (the arrangement used being that described in Part I, §5); it will be seen that, in conformity with theory, a particular point (such as P') on the hyperbolic segment O_1A_1 is extinguished—this point representing the direction where the incident elliptic vibration is propagated unchanged. When the coupled retardation plates are rotated around together by 90° (so that X_k becomes the *fast* vibration-direction of the first retardation plate), a corresponding point on the hyperbolic segment O_1A_1' is extinguished—as seen in Fig. 10. In Figs. 11 and 12 (Plate XII) the coupled polaroids have been turned so that in both cases the vibration-direction of the first polaroid is parallel to $O'A_2'$ (represented by A_2' on the Poincaré sphere); the slow vibration-direction of the first retardation plate lies along the axial plane in Fig. 12 but perpendicular to it in Fig. 11. In the former case the point near O_1 which is extinguished lies on the hyperbolic segment O_1A_2, while in the latter (Fig. 11) it lies on O_1A_2'. In all the four photographs (Figs. 9–12, Plate XII) the extinguished points should lie on a curve of constant linear birefringence —a point which is difficult to confirm exactly. It was however verified that when the experiments were repeated with mica plates of lower retardation, the extinguished spots had in all cases moved outwards along the respective hyperbolic arcs. All these observations confirm the theoretical results stated in this section.

§7. SINGULAR AXES

We shall now consider directions of propagation for which the principal planes of linear birefringence are equally inclined to the axial plane. Considering first a point on the hyperbolic segment O_1M (Fig. 3 *b*, text), the orientation of the principal plane of linear birefringence OX_r will be parallel to O'M, and will be represented by the point M on the Poincaré sphere (Fig. 4 *a*, text). Hence for this direction of propagation the state B (representing the slower wave in the absence of dichroism) will be a point on the meridian C_lM, at latitude $2\omega_1$; and the elliptic birefringence Δ in the absence of dichroism will [according to P–*a* Eq. (1)] be equal to $|2\rho|$ cosec $2\omega_1$. The great circle CX_kC' is drawn having B and B′ as its poles. The arc X_kB is a quadrant, and from the condition that the angle it subtends at P_a should be a right angle, it may be seen geometrically [or from P–*a*, Eq. (5)] that P_a

must lie either on the arc CX_k ($2\phi_a = \frac{1}{2}\pi$) or on the meridional arc BC ($2\psi_a = \frac{1}{2}\pi$). The former situation is illustrated in Fig. 4 *a*, text, and holds when the direction under consideration is still sufficiently close to the axial direction O_1 for k to be greater than Δ. It may be shown [using Eq. (1) above, and P-*a*, Eq. (4)] that the states P_a and P_b are the points of intersection of the great circular arc X_kCY_k with the small circle $E_2A_1E_1$ of spherical radius MA_1 drawn about M as centre. As we proceed outwards from the optic axis O_1 along the segment O_1M, Δ increases while at the same time the latitude $2\omega_1$ of the point B decreases: thus the states P_a and P_b which originally coincide with A_1 and A_2 move along the small circle towards the state E_1.

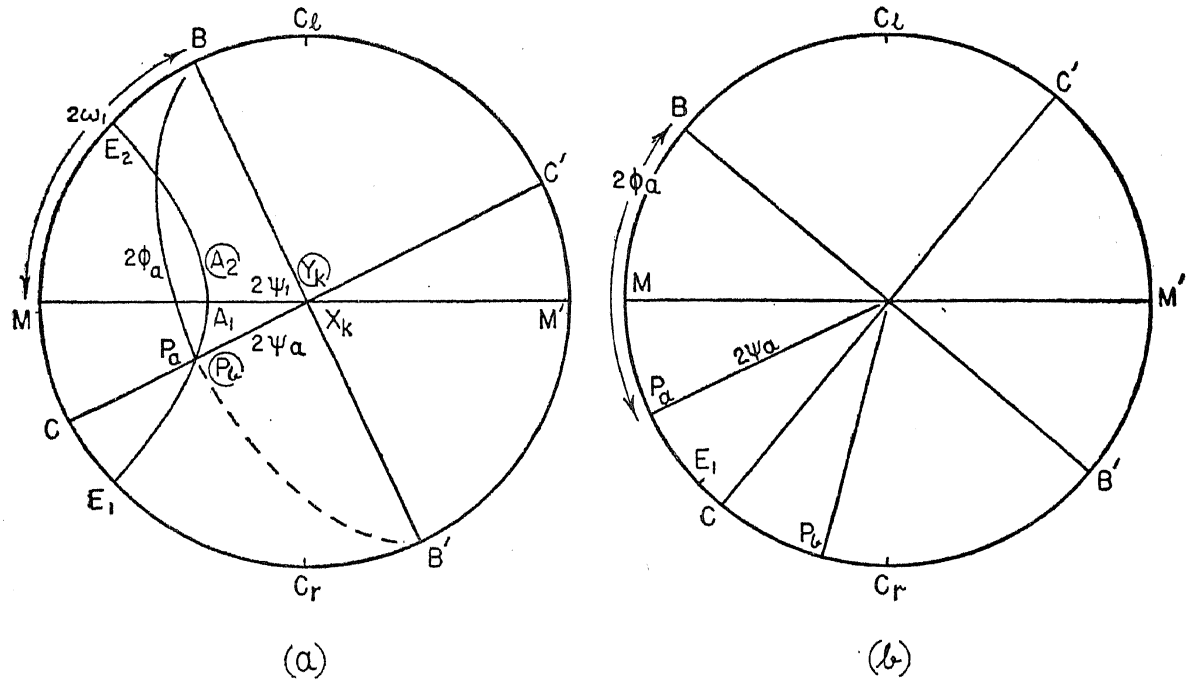

TEXT-FIG. 4. Construction for determining the states of polarisation of the propagated waves (*a*) for points on O_1S_1 in Fig. 3 *b*, text, (*b*) for points on S_1M in Fig. 3 *b*, text. The states E_1 and E_2 are respectively propagated unchanged along the singular axes S_1 and S_2.

In Fig. 3 *b*, text, S_1 denotes the direction of propagation on the segment O_1M for which Δ has become equal to k: since $\Delta = |2\rho| \operatorname{cosec} 2\omega_1$, it may be seen from Eq. (1) that for this direction $\omega_1 = \psi_1$ so that the point C of Fig. 4 *a*, text, now coincides with E_1. *For the direction of propagation S_1 there are no longer two distinct states of polarisation which can be propagated unchanged* since both states P_a and P_b have coalesced with the state represented by E_1 on the Poincaré sphere. Thus there is only *one* state of vibration which can be propagated without change of form along the '*singular*

axis' S_1—as may be directly shown from P-*a*, Eqns. (4) and (5) by setting $k = \Delta$, and $2\chi' = \frac{1}{2}\pi$. As we proceed further outwards along the segment O_1M, we will have $\Delta > k$; the states of polarisation P_a and P_b of the waves become again separate, moving from E_1 towards M and M′ respectively, along the arcs joining E_1 to these points. Thus Fig. 4 *b*, text, illustrates the position of the states P_a and P_b for a direction of propagation on the segment S_1M. The variation of the states of polarisation of the waves as we proceed outwards along O_1M' may be similarly traced on the Poincaré sphere using the relations stated in the concluding paragraph of §5 *c*. The direction S_2 for which $k = \Delta$, is again a singular axis where *only* the state of polarisation E_2 can be propagated unchanged—the points E_2 and E_1 being related to one another by reflection about the equatorial plane of the sphere.

The results proved above have been expressed in terms of the Poincaré sphere. They may be easily translated into physical terms, and the actual variation of the states of polarisation of the waves along the segments O_1M and O_1M' has been depicted (in an exaggerated form) in Fig. 3 *b*, text. The single wave which can be propagated along the singular axis S_1 differs from that which can be propagated along S_2, only in the sense of description; but both states are elliptically polarised and are not orthogonal to one another—unlike the case in inactive absorbing crystals.

Fig. 13 (Plate XIII) shows the photograph obtained with an elliptic polariser and a crossed elliptic analyser (*see* Part I, §5), the elliptic polariser being adjusted to produce the state of polarisation E_2 which can be propagated unchanged along the singular axis S_2; the vibration-direction of the first polaroid was kept along the direction $O'A_2$ (which is represented by the state A_2 in Fig. 4 *a*, text), this being followed by a quarter-wave plate with its slow axis along O′M (represented by M in Fig. 7). The singular axis S_2 and a corresponding singular axis associated with the other optic axis, appear extinguished in Fig. 13, Plate XIII. By turning the coupled polaroids so that the vibration-direction of the first polaroid is parallel to $O'A_1$ we observe the figure presented with an elliptic polariser E_1 and a crossed elliptic analyser. Fig. 14 shows this photograph, the singular axis S_1 and a corresponding singular axis associated with the optic axis O_2, being extinguished. (The singular axes have been indicated by spots in Figs. 13 and 14.) Fig. 15 shows the photograph obtained with the elliptic analyser removed in the arrangement of Fig. 14. This has to be compared with Fig. 16 which has been obtained by turning the polaroid by 90° relative to its orientation in Fig. 15. In Fig. 16, therefore, the elliptic vibration incident on the crystal is *orthogonal* to that which alone can be propagated unchanged along the singular axis S_1. Nevertheless, *the light incident along*

this singular direction is not reflected away; in fact the intensity of the light emerging along S_1 in Fig. 16, Plate XIII is *greater* than in Fig. 15, though in the latter case the incident vibration is in a state which is propagated unchanged along S_1. We need not enter into the explanation of this phenomenon, since it follows exactly along the lines given previously for a corresponding phenomenon observed in *inactive* absorbing crystals;[5,6] the principle of superposition must be directly applied and the vibration incident along the singular direction S_1 in Fig. 16, Plate XIII will be propagated with a progressive change in its state of polarisation.

For any direction of propagation lying within the small strip $S_1O_1S_2$ (Fig. 3 *b*, text) the refractive indices of the waves will be equal according to P–*a*, Eq. (13), since for such a direction we have, $2\phi_a = \frac{1}{2}\pi$ from Fig. 4 *a*, text; the absorption coefficients of the waves will however be different according to P–*a*, Eq. (10), tending to equality only as the singular directions are approached. For the remaining points on the hyperbolic branch MO_1M', it is the refractive indices of the two waves which are different, the difference increasing from zero as we proceed outwards from the singular directions; while *the absorption coefficients are equal for this zone of directions* since $2\psi_a = \frac{1}{2}\pi$ from Fig. 4 *b*. Now in all the interference figures observed when the states of the polariser and analyser are crossed, the minima of the ring system should appear perfectly dark only along the zones where the absorption coefficients of the waves are equal [P–IV,[6] Eq. (21)]. Thus Figs. 1–6 and Figs. 9–14 confirm that the absorption coefficients of the waves are equal for points on the rectangular hyperbola one branch of which has been marked MO_1M' (the small strips joining the singular axes being excepted). This is also confirmed by the appearance of Brewster's brushes along the same zones—a feature which is to be theoretically expected from P–IV, Eq. (11) (following the same reasoning as for inactive absorbing crystals[7]), since the sum of the absorption coefficients of the waves may be taken to be constant over the region under consideration according to P–*a*, Eq. (9).

§8. Phenomena with Polariser alone and Analyser alone

In a previous publication[6] it has been explained quite generally that in crystals where the waves propagated along any direction are non-orthogonally polarised, interference rings should be exhibited with a polariser alone in front of the plate (*i.e.*, with no analyser); and also with an analyser alone behind the plate, the incident light being unpolarised. The ' idiophanic rings ' of the former class are exhibited in Figs. 17–20, for various settings of the linear polariser as the latter is turned in a clockwise sense—starting with the setting for which the vibration-direction is along the axial plane, as in

Fig. 17. Similarly, Figs. 21–24 show the idiophanic rings for various settings of a linear analyser as the latter is turned in an *anti*-clockwise sense, starting with the setting of Fig. 21, where the vibration-direction lies along the axial plane. In the observations with a polariser alone it was found that two hyperbolic brushes passing through the optic axes were formed in the setting of Fig. 18, Plate XIII, for which the vibration-direction of the polaroid was parallel to $O'A_2$ in Fig. 1, text; but Fig. 24 obtained with an analyser alone in the same setting is entirely different. So also in observations with an analyser alone, two hyperbolic brushes passing through the axial directions formed in the setting of Fig. 22, Plate XIV, where the vibration-direction of the polaroid was parallel to $O'A_1'$, in Fig. 1, text; but Fig. 20, obtained with a polariser alone in the same setting, is entirely different from Fig. 22.

Thus *the effects presented with a linear polariser alone are, in general, not the same as with a linear analyser alone* in the same setting. This proves that the non-orthogonally polarised states propagated along a general direction *cannot* be of the special type propagated in inactive absorbing crystals (*see* P–IV, §7).

It is physically understandable that the setting of the polaroid at which an optic axial direction, *e.g.*, O_1 appears darkest, differs according as whether the polaroid is set before or after the plate. In the former case the polariser-vibration would have to be parallel to $O'A_2$, *i.e.*, to the vibration-direction of the more heavily absorbed wave propagated along O_1; while in the latter case the analyser-vibration has to be parallel to $O'A_2'$ so that it will be *crossed* with respect to the vibration-direction of the *less* absorbed wave propagated along O_1. It remains to explain why at these settings, we find a whole zone of directions, represented by the hyperbolic brushes in Figs. 18 and 22, which appear as dark as the optic axial directions. For this purpose it must be remembered that the coefficients of linear dichroism as well as the orientations of the principal planes of linear dichroism are taken as constant over the region considered; so that the absorption coefficient of a wave propagated along any direction becomes purely a function of its state of polarisation: more precisely, *the absorption coefficient is purely a function of the angular distance* 2ϕ *of this state from* X_k, on the Poincaré sphere [P–*a*, Eq. (9)]. For the zone of directions of the rectangular hyperbola, one branch of which is marked $A_2O_1A_2'$ (Fig. 1, text), the state of polarisation of one of the waves is constant—being linearly polarised parallel to $O'A_2$ (§4). Hence when the vibration-direction of the polariser lies along $O'A_2$, the light suffers equal absorption all along this zone of directions, giving rise to hyperbolic brushes of uniform depth as in Fig. 18.

Similarly, consider any direction of propagation such as P′ on the rectangular hyperbola, one branch of which is $A_1O_1A_1'$. For any such direction the absorption coefficient of the more heavily absorbed wave will always be equal to the absorption coefficient (α_2 say) of the more heavily absorbed wave propagated along an optic axis such as O_1; this follows because according to §6, both these states (P_b and A_2) lie on a small circle with X_k as centre, and hence are at the same angular distance from X_k on the Poincaré sphere (Fig. 4 *a*, text). When unpolarised light of unit intensity is incident on a direction such as P′ the two non-orthogonally polarised waves (in states A_1 and P_b) into which it is split will both have initial intensities equal to $\frac{1}{2}\sec^2\frac{1}{2}A_1'P_b$ (*see* reference 8, §7). When a polaroid is kept behind the plate with its vibration-direction parallel to $O'A_1'$ it completely crosses out the less absorbed wave emerging along the direction P′ since this wave is linearly polarised parallel to $O'A_1$ (§4); a fraction $\cos^2\frac{1}{2}A_1'P_b$ of the intensity of the more heavily absorbed wave will however be transmitted by the analyser along the direction P′. Thus in the idiophanous figure observed with the analyser-vibration parallel to $O'A_1'$, the intensity of all points such as P′ (lying on the rectangular hyperbola, one branch of which is $A_1O_1A_1'$) will be equal to $\frac{1}{2}\exp(-\alpha_2 d)$, *i.e.*, it will be the same as the intensity of the axial direction in Fig. 18, Plate XIII. This explains the occurrence of the dark brushes in Fig. 22.

It has been shown in P–IV, §7, that the idiophanous figures presented with a polaroid set before or after the plate will not differ *if* the following condition is satisfied; on the Poincaré sphere, the angular distances of the points P_a and P_b (representing the states propagated along any direction) from the point representing the vibration-direction of the polaroid, should be supplements of one another. From the results of P–*a*, §4, it may be seen that this condition will be satisfied in the *particular* cases when the vibration-axis of the polaroid coincides with X_k or Y_k, *i.e.*, with one of the principal planes of linear dichroism $O'X_k$ or $O'Y_k$. This explains why Figs. 17 and 21 appear identical, as also Figs. 19 and 23.

It will be noted from the photographs that the idiophanous figures presented with a linear polariser at a setting of $+\theta$ to the axial plane is similar in some respects to that presented with a linear analyser at the setting $(-\theta)$ to the axial plane—the figures in the two cases being in fact related merely by reflection about the vertical line Y_kY_k' (*Compare* Fig. 18 with Fig. 22, and Fig. 20 with Fig. 24). This may be explained using the results stated at the end of §5 *c*; the intensity at the point P (δ, χ) with the polariser-vibration at $+\theta$ to $O'X_k$ [being given by P–IV, Eq. (6)] may be shown

to be equal to the intensity at P (δ, $-\chi$) with the analyser-vibration at ($-\theta$) to $O'X_k$ [as obtained from P–IV, Eq. (16)].

Finally it may be mentioned that observations with a polariser alone and with an analyser alone readily revealed a characteristic difference in the behaviour of a *left*-rotating sector (occurring in another basal plate). The orientations of the polaroid at which the brush formed in the two cases showed that the azimuth of the linearly polarised states propagated along the optic axes lay in the *positive* quadrant—as is to be expected from theory (P–*a*, §8 *b*).

The author is highly indebted to Prof. Sir C. V. Raman, for his unfailing interest in the present work.

SUMMARY

Using a wavelength (λ 5890) for which the linear dichroism of the amethystine sector is appreciable ($k > |2\rho|$), twenty-four interference figures are reproduced confirming in detail the theory of light propagation in absorbing crystals possessing optical activity.[1] Unlike the behaviour in transparent crystals, the idiophanic interference figures seen with a polariser alone in front of the plate differ in general from those presented with an analyser alone behind the plate in the same setting. The existence of four singular axes, one on either side of each optic axis, is shown: along each singular axis only *one* (elliptically) polarised wave—and not two—can be propagated without change of form.

REFERENCES

1. Pancharatnam, (P–*a*) .. *Proc. Ind. Acad. Sci.*, 1957, **46 A**, 280.
2. ———— .. *Ibid.*, 1956, **44 A**, 247.
3. Johannsen .. *Manual of Petrographic Methods*, McGraw-Hill, 1918, 440.
4. Wooster .. *A Text-book on Crystal Physics*, Cambridge, 1938, 141.
5. Pancharatnam .. *Proc. Ind. Acad. Sci.*, 1957, **46 A**, 86, 235.
6. ————, (P–IV) .. *Ibid.*, 1957, **45 A**, 2.
7. Pockels .. *Lehrbuch der Kristalloptik, Teubner*, 1906, 421.
8. Pancharatnam .. *Proc. Ind. Acad. Sci.*, 1956, **44 A**, 398.
9. ———— .. *Ibid.*, 1954, **40 A**, 196.
10. Dove .. *Farbenlehre*, 1853, Seite 251.
11. Liebisch .. *Ber. Berl. Akad.*, 1916, **36**, 870.
12. Leitz and Munchberg .. *Neues Jb. Mineral*, 1956, **10**, 217.

APPENDIX

It was shown in a previous investigation[9] on amethystine quartz that the approximate orientation of the absorption ellipsoid could be derived purely from observations on the pleochroism made at appreciable inclinations to the *c*-axis. As regards the observations in convergent light and their explanation described in that paper, they have no doubt to be supplemented by the account given in the present paper—but this does not alter the conclusions already drawn from them. Thus the present paper establishes rigorously that if we consider the section of the absorption ellipsoid normal to the *c*-axis, then the major semi-axis of the elliptic section coincides with the obtuse-bisectrix—*which in turn coincides with an* a-*axis of quartz*. The method, previously used, of determining the orientations of these principal axes for less intensely coloured areas by observations with a single polaroid* may also be rigorously justified using the results stated at the end of §8. Very significant too is the fact that the intensity of Brewster's brushes (Part I, Fig. 5, Plate IX) appears symmetrical about the plane Y_kY_k' but not about the axial plane. This indicates that the plane Y_kY_k' (normal to the *a*-axis mentioned) is a plane of symmetry of the absorption ellipsoid—though this is not true of the axial plane. This is confirmed by the appearance of Brewster's brushes in white light: the two brushes below the axial plane appear bluish purple towards the border of the figure while those above are of a deeper reddish purple colour. The explanation of this is that there are two colour axes in the symmetry plane Y_kY_k' which lie on either side of the *c*-axis at approximately 45° to it—the colours for vibrations along these axes being blue and deep red respectively.

According to the results of our previous investigation[9] the amethystine material occurring in the quartz can take up one of several discrete optic orientations all consistent with the description given above. An overlap of amethystine material of different optic orientations can be produced by one or more of the following three factors: (1) overlap of sectors associated with different rhombohedral faces, (2) optical twinning in which the different twin members are of opposite handedness, (3) electrical twinning in which the electrical axes of the different twin members are in opposite orientation. The main difficulty of studying the pleochroism of amethyst in any random section plate is that optical twinning of an interpenetrant variety occurs

---

* Brewster's brushes had been referred to in our earlier paper[9] as the idiophanous figure —a term reserved in the present paper for the figure presented with a polariser or analyser alone in conformity with the more prevalent usage.

extensively. Some of the investigations of Dove[10] and Liebisch[11] are of value in interpreting the interference figures in such optically twinned areas, but they do not directly concern the investigations presented in this paper.

Subsequent to our previous publication on the pleochroism of amethyst there has appeared an interesting paper by Lietz and Munchberg[12] dealing with the same problem. The difference between their conclusions and ours certainly appears to raise the interesting possibility of the existence of different species of amethyst with entirely different optical chracteristics.† Nevertheless, it would be difficult to decide how far there is real disagreement between our conclusions and the experimental part of their observations. The existence of pleochroism along the *c*-axis is common ground: and because the subject of refractive index and absorption are closely interlinked by dispersion theory, it follows that the index ellipsoid could not be strictly uniaxial for all wavelengths. In view of this fact their statement that amethyst possesses uniaxial symmetry can only be taken to mean that the index ellipsoid is *very nearly* uniaxial. With this we are in complete agreement, if we restrict ourselves to sectors of moderate colouration such as they have chosen. The mean absorption coefficient of the sector which was used by them for observing the interference figure was about $0{\cdot}75\ \text{cm.}^{-1}$ for wavelengths near the absorption maximum; whereas for the sector used in the present investigation the *difference* k between the absorption coefficients for vibrations parallel to $O'Y_k$ and $O'X_k$ is itself about 15 times that value (*see* §3). Using the same sector as employed in the present investigation the absorption spectrograms for vibrations along the three colour axes had been reproduced in our previous paper: though the actual wavelengths of the absorption maxima were only qualitatively located, the spectrograms clearly showed the difference in intensity and position of the absorption maxima, especially for the two main absorption axes (red and blue). The latter difference would not have been present if there had been electrical twinning. Also—considering the great breadth of the absorption band in amethyst—we do not know whether the shift of the absorption maxima could have been easily detected if the sector had not been so intensely coloured, and if the vibrations had not been polarised exactly along the colour axes. Regarding this point, however (*viz.*, the orientation of the principal axes of the absorption ellipsoid), the conclusions of Leitz and Munchberg differ from ours. This would again appear to point more clearly to a fundamental difference in the nature of the amethystine material investigated in

† The material studied by us were mainly from Hyderabad, but included a few uncut specimens from Uruguay.

FIG. 1

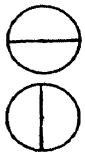

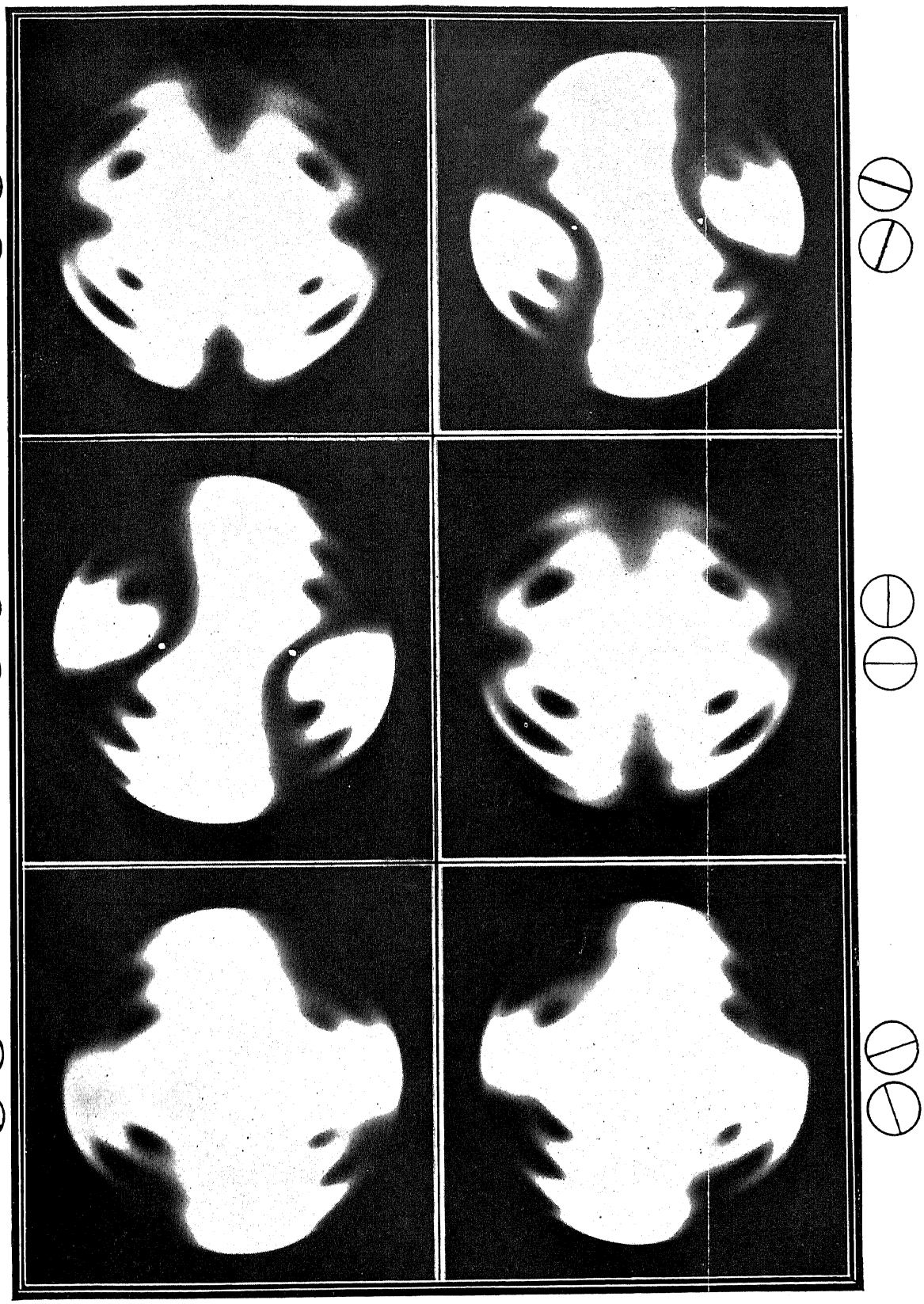

FIG. 2

FIG. 3

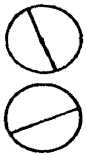

FIG. 4

FIG. 5

FIG. 6

FIGS. 1–6

Interference Figures observed between crossed polaroids.

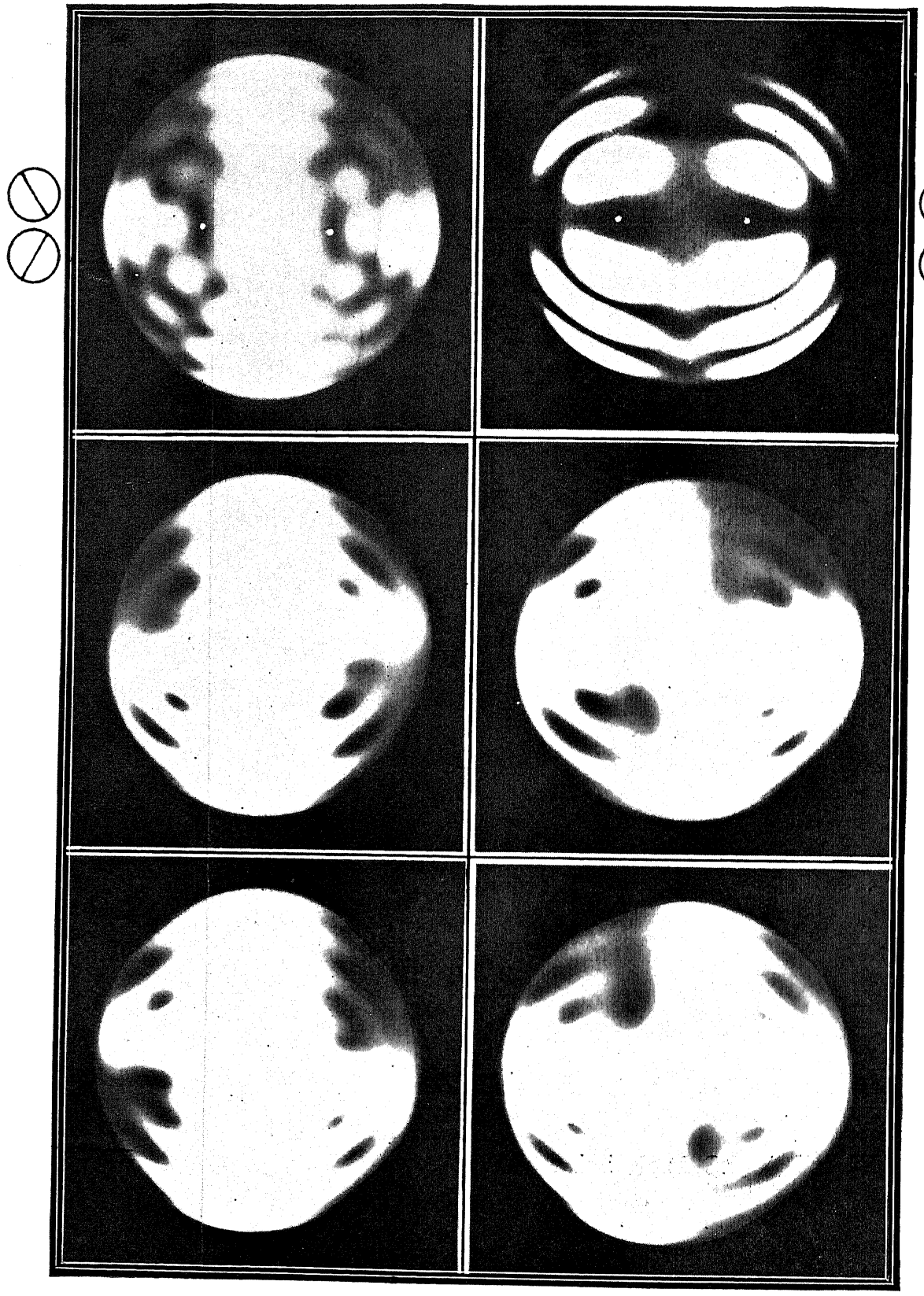

FIG. 7 FIG. 8 FIG. 9 FIG. 10 FIG. 11 FIG. 12

FIGS. 7–12

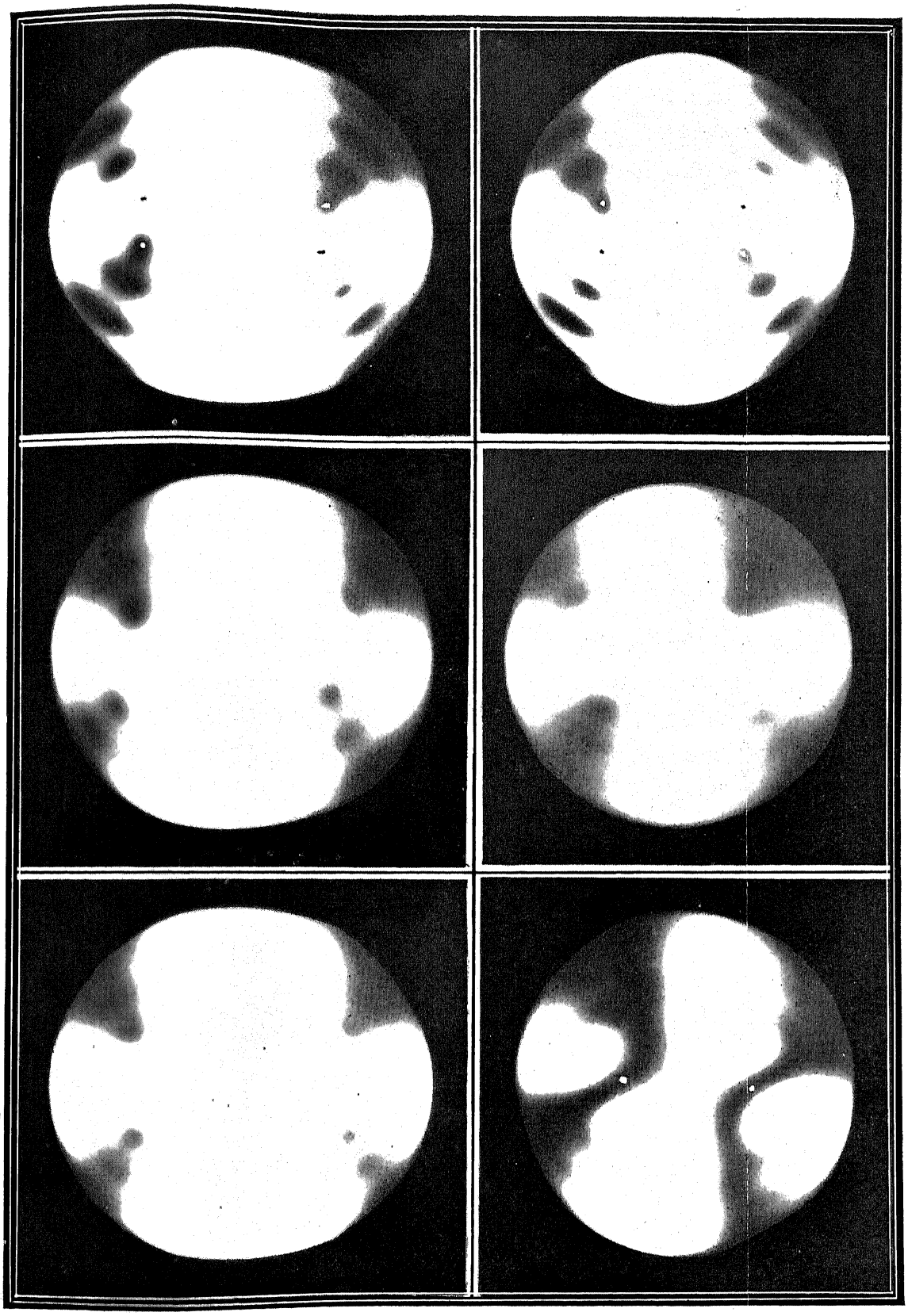

FIG. 13 FIG. 14

FIG. 15 FIG. 16

G. 17 FIG. 18

FIGS. 13-18

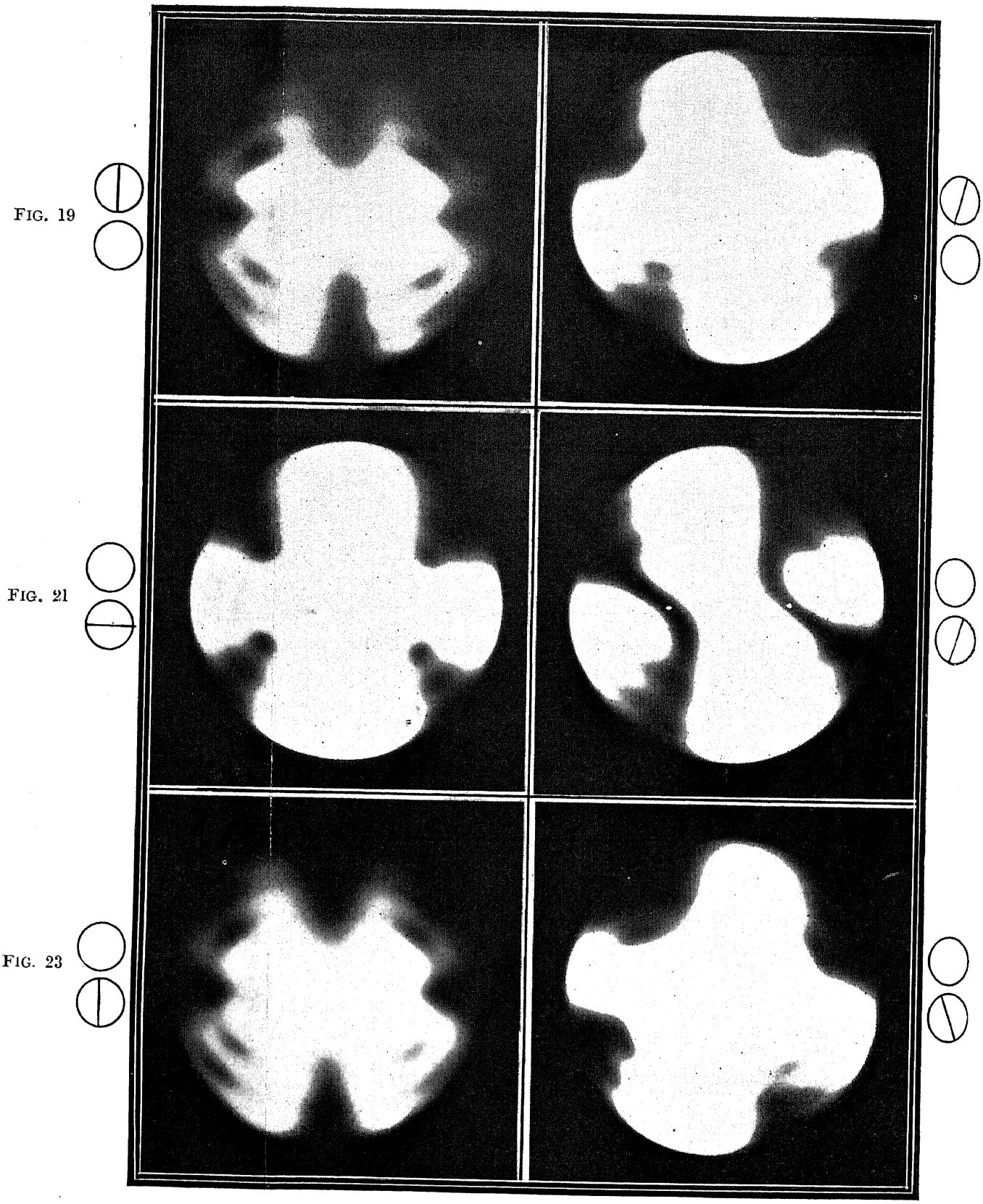

FIGS. 19–24

Phenomena with polariser alone, and analyser alone.

the two cases. But before this can be asserted with any confidence the following fact must also be taken into account: that for finding the orientation of the principal axes of the absorption ellipsoid it is *not* sufficient to measure the absorption for three mutually perpendicular vibrations. This has been done by Leitz and Munchberg by observations through the faces $(10\bar{1}0)$ and $(1\bar{2}10)$. (The observations through the basal section are of course only useful for showing the absence of uniaxial symmetry, unless account is taken theoretically of the presence of optical activity.)